An IMM Algorithm for Tracking Maneuvering Vehicles in an Adaptive Cruise Control Environment

Yong-Shik Kim and Keum-Shik Hong*

Abstract: In this paper, an unscented Kalman filter (UKF) for curvilinear motions in an interacting multiple model (IMM) algorithm to track a maneuvering vehicle on a road is investigated. Driving patterns of vehicles on a road are modeled as stochastic hybrid systems. In order to track the maneuvering vehicles, two kinematic models are derived: A constant velocity model for linear motions and a constant-speed turn model for curvilinear motions. For the constant-speed turn model, an UKF is used because of the drawbacks of the extended Kalman filter in nonlinear systems. The suggested algorithm reduces the root mean squares error for linear motions and rapidly detects possible turning motions.

Keywords: Adaptive cruise control, constant-speed turn model, extended Kalman filter, hybrid estimation, interacting multiple model, nonlinear filtering, unscented Kalman filter.

1. INTRODUCTON

Recently, the majority of automobile companies are developing various driver assistance systems to increase vehicle safety and alleviate driver workload. The driver assistance systems include adaptive cruise control (ACC), lane-keeping support, collision warning and collision avoidance, and assisted lane changes. The effectiveness of these driver assistant systems depends on the interpretation of the information arriving from sensors, which provide details of the surrounding vehicle environment and of the driver-assisted vehicle itself. In particular, all these systems rely on the detection and subsequent tracking of objects around the vehicle. Such detection information is provided by radar, lidar, and vision sensor. The assistance systems mentioned above have certain objectives that their controllers try to meet. Before a controller can make a decision that enables the driver to feel natural, the motion of the surrounding object must be properly interpreted from the available sensor information [2].

Manuscript received March 10, 2004; revised July 10, 2004; accepted July 20, 2004. Recommended by Editor-in-Chief Myung Jin Chung. This work was supported by the Ministry of Science and Technology of Korea under a program of the National Research Laboratory, grant number NRL M1-0302-00-0039-03-J00-00-023-10.

Yong-Shik Kim is with the Department of Mechanical and Intelligent Systems Engineering, Pusan National University, San 30 Jangjeon-dong Gumjeong-gu, Busan 609-735, Korea (e-mail: immpdaf@pusan.ac.kr).

Keum-Shik Hong is with the School of Mechanical Engineering, Pusan National University, San 30 Jangjeon-dong Gumjeong-gu, Busan 609-735, Korea (e-mail: kshong@pusan.ac.kr).

* Corresponding author.

Fig. 1 shows the configuration of an ACC system. The ACC system consists of a driver interface, a radar sensor which measures both the distance and speed of preceding vehicles, a controller which controls both throttle and brake actuators, and actuators [17]. The ability to accurately predict the motion of preceding vehicles in the ACC environment can improve the controller's ability to adapt smoothly to the behavior of those vehicles preceding it. This ability to predict motions is dependent on how well the radar of an ACC vehicle can track other vehicles. In order to track other vehicles using the object information obtained from multiple sensors, tracking techniques based on the Bayesian approach are usually used [1]. The tracking of a maneuvering target is already well-established topic in the target tracking literature.

Techniques for tracking maneuvering targets are used in many tracking and surveillance systems as well as in applications where reliability is the main concern [1,6,13,14]. In particular, tracking a maneuvering target using multiple models can provide better performance than using a single model. A number of multiple model techniques to track a maneuvering target have been proposed in the literature: the multiple-model algorithms [13], the interacting multiple model (IMM) algorithm [1,14,15, 23], the adaptive IMM [7,18], the fuzzy IMM [3,16],

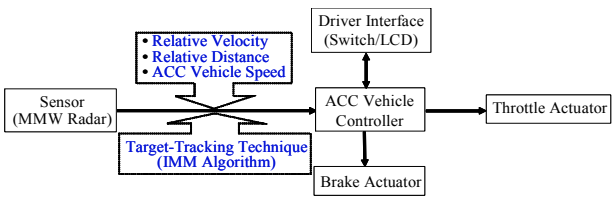

Fig. 1. Configuration of the ACC system.

and others.

Generally, target motion models can be divided into two subcategories: the uniform motion model and the maneuvering model. A maneuvering target moving at a constant turn-rate and speed is usually modeled as a maneuvering model, and called a coordinated turn model [1,4,5,7,14,18].

For application to air traffic control, a fixed structure IMM algorithm with a single constant velocity model and two coordinated turn models was analyzed [14]. And, for the tracking of a maneuvering target, a validation method of a new type of flight mode was presented in [19]. Nabaa and Bishop [19] validated a non-constant speed coordinated turn aircraft maneuver model by comparing their model with the classic Singer maneuver model and a constant-speed coordinated turn model using actual trajectories. Semerdjiev and Mihaylova [22] discussed variable- and fixed-structure augmented IMM algorithms, whereas a fixed-structure algorithm only was discussed in [14], and applied to a maneuvering ship tracking problem by augmenting the turn rate error.

The drawbacks of the interacting multiple model algorithms using extended Kalman filters (IMM-EKF) are as follows. First, the EKF approximates a non-Gaussian density with a Gaussian density [24]. Second, the IMM approximates the Gaussian mixture with a single Gaussian density. If these assumptions break down, the IMM-EKF may diverge. In this paper, because of these drawbacks of the IMM-EKF, an unscented Kalman filter (UKF) [8,21], replacing the EKF, is used for the curvilinear model. The algorithm itself uses the same IMM logic, but the model-matched EKF is replaced by the model-matched UKF. The objective of this paper is to design an UKF for curvilinear motions in an IMM algorithm to track a maneuvering vehicle for the driving of an ACC vehicle on a road.

The contributions of this paper are as follows. First, the IMM algorithm is provided as a driving algorithm for an ACC vehicle in driving on a road. Second, two kinematic models for the possible driving patterns of vehicles are derived: A constant velocity model for linear motions and a constant-speed turn model for curvilinear motions are discussed. Third, for the constant-speed turn model, an UKF is used because of the drawbacks of the EKF. Fourth, the suggested algorithm reduces the root mean squares error in the case of rectilinear motions and detects the occurrence of maneuvering quickly in the case of turning motions.

This paper is organized as follows: In Section 2, we provide the various driving patterns of vehicles. A stochastic hybrid system is formulated, and two kinematic models are discussed. In Section 3, we compare an UKF with an EKF for a constant- speed turn model in an IMM algorithm. In Section 4, we evaluate the performance of these filters using Monte Carlo simulation under the various driving patterns. Section 5 concludes the paper.

2. PROBLEM FORMULATION

In this section, after analyzing the driving patterns of a vehicle on a road, a stochastic hybrid system in the form of an IMM algorithm for tracking the preceding vehicle using sensors (radar, lidar, sonar, vision, etc) is formulated. Also, two kinematic models representing the analyzed driving patterns are introduced.

2.1. Driving patterns

Fig. 2 depicts the various driving patterns of a vehicle: straight line and curve, cut-in/out, u-turn, and interchange. All of these patterns can be represented by a combination of a constant-velocity rectilinear motion, a constant-acceleration rectilinear motion, a constant angular velocity curvilinear motion, and a constant angular acceleration curvilinear motion. As kinematic models for describing these motions, two stochastic models will be investigated: one for rectilinear motion and the other for curvilinear motion. These typical driving patterns are described briefly as follows:

i) Straight line and curve: In this situation, the ACC vehicle tracks a preceding vehicle that follows straight lines and curves on a curved road [10,20].

ii) Cut-in/out: The cut-in/out indicates the situation in which a maneuvering vehicle cuts in (or out) to (or from) the lane while the ACC vehicle is tracking other vehicle. In this situation, the tracking of up to three surrounding vehicles is assumed: one in front, one to the left, and one to the right. In this case, the target vehicle changes its motion from a rectilinear motion to a curvilinear motion and then back to a rectilinear motion.

iii) U-turn: This situation occurs when the target vehicle changes its driving direction by $180°$. The u-turn consists of three routes as follows: The target vehicle moves rectilinearly, undergoes a uniform circular turning of up to $180°$ with a constant yaw rate, and then converts to a rectilinear motion in the opposite direction.

iv) Interchange: When the ACC vehicle is passing through an interchange, the target vehicle undergoes a 3-dimensional motion. The target vehicle moves rectilinearly, undergoes a uniform circular turning of up to $270°$ with a constant yaw rate, and then converts to a rectilinear motion. In this paper, passing an interchange will be simplified by a 2-dimensional motion.

It will be shown in the sequel that a constant-velocity model will capture both constant velocity and acceleration rectilinear motions without and with an

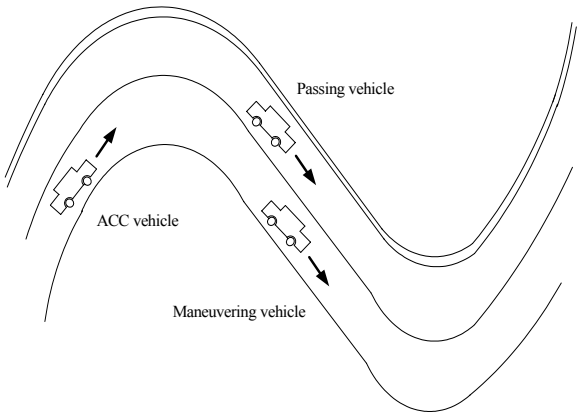

(a) straight line and curve

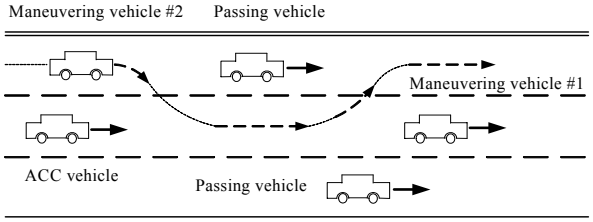

(b) cut-in/out

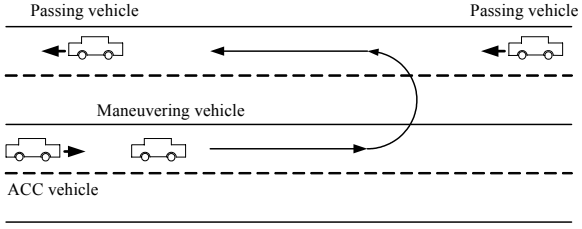

(c) u-turn

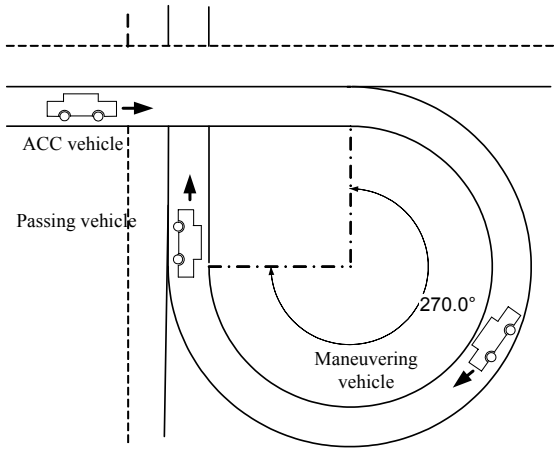

(d) interchange

Fig. 2. Various driving patterns of vehicles.

additional noise term, respectively. On the other hand, a constant-speed turn model will cover both constant angular velocity and angular acceleration curvilinear motions without and with a noise term, respectively.

2.2. Stochastic hybrid system

Following the work of Li and Bar-shalom [14], a stochastic hybrid system with additive noise is considered as follows:

$$x(k) = f[k-1, x(k-1), m(k)] + g[k-1, x(k-1), \nu[k-1, m(k)], m(k)] \quad (1)$$

with noisy measurements

$$z(k) = h[k, x(k), m(k)] + w\ [k, m(k)], \quad (2)$$

where $x(k) \in \Re^{n_x}$ is the state vector including the position, velocity, and yaw rate of the vehicle at discrete time k, $m(k)$ is the scalar-valued modal state (driving mode index) at instant k, which is a homogeneous Markov chain with probabilities of transition given by

$$P\{m_j(k+1) \mid m_i(k)\} = \pi_{ij}\ , \qquad \forall m_i, m_j \in \mathrm{M}, \quad (3)$$

where $P\{\cdot\}$ denotes the probability and M is the set of modal states, that is, constant velocity, constant acceleration, constant angular rate turning with a constant radius of curvature, etc. The considered system is hybrid since the discrete event $m(k)$ appears in the system. In the driving of ACC vehicle, $m(k)$ denotes the driving mode of the preceding vehicle, in effect during the sampling period ending at k, that is, the time period $(t_{k-1}, t_k]$. The event for which a mode m_j is in effect at time k is denoted as

$$m_j(k) \overset{\Delta}{=} \{m(k) = m_j\}. \quad (4)$$

$z(k) \in \Re^{n_z}$ is the vector-valued noisy measurement from the sensor at time k, which is mode-dependent. $\nu[k-1, m(k)] \in \Re^{n_\nu}$ is the mode-dependent process noise sequence with mean $\bar{\nu}[k-1, m(k)]$ and covariance $Q[k\text{-}1,\ m(k)]$. $w\ [k, m(k)] \in \Re^{n_z}$ is the mode-dependent measurement noise sequence with mean $\bar{w}[k, m(k)]$ and covariance $R[k, m(k)]$. Finally f, g, and h are nonlinear vector-valued functions.

2.3. Two kinematic models

The concept of using noise-driven kinematic models comes from the fact that noises with different levels of variance can represent different motions. A model with high variance noise can capture maneuvering motions, while a model with low variance noise represents uniform motions. The multiple-models approach assumes that a model can immediately capture the complex system behavior better than others.

Two kinematic models for rectilinear and curvilinear motions are now derived. First, assuming that accelerations in the steady state are quite small (abrupt motions like a sudden stop or a collision are not covered), linear accelerations or decelerations can be

reasonably well covered by process noises with the constant velocity model. That is, the constant velocity model plus a zero-mean noise with an appropriate covariance representing the magnitude of acceleration can handle uniform motions on the road. In discrete-time, the constant velocity model with noise is given by

$$x(k)=\begin{bmatrix}1 & T & 0 & 0\\ 0 & 1 & 0 & 0\\ 0 & 0 & 1 & T\\ 0 & 0 & 0 & 1\end{bmatrix}x(k-1)+\begin{bmatrix}\frac{1}{2}T^2 & 0\\ T & 0\\ 0 & \frac{1}{2}T^2\\ 0 & T\end{bmatrix}\nu(k-1), \quad (5)$$

where T is the sampling time (i.e., 0.01 sec in this paper), $x(k)$ is the state vector including the position and velocity of the preceding vehicle in the longitudinal (ξ) and lateral (η) directions at discrete time k, that is,

$$x(k)=[\xi(k)\ \ \dot{\xi}(k)\ \ \eta(k)\ \ \dot{\eta}(k)]' \quad (6)$$

with ξ and η denoting the orthogonal coordinates of the horizontal plane; and ν is a zero-mean Gaussian white noise representing the accelerations with an appropriate covariance Q. If $\nu(k)$ is the acceleration increment during the k th sampling period, the velocity during this period is calculated by $\nu(k)T$, and the position is altered by $\nu(k)T^2/2$.

Second, a discrete-time model for turning is derived from a continuous-time model for the coordinated turn motion [1, p. 183]. A constant speed turn is a turn with a constant yaw rate along a road of constant radius of curvature. However, the curvatures of actual roads are not constant. Hence, a fairly small noise is added to a constant-speed turn model for the purpose of capturing the variation of the road curvature. The noise in the model represents the modeling error, such as the presence of angular acceleration and non-constant radius of curvature. For a vehicle turning with a constant angular rate and moving with constant speed (the magnitude of the velocity vector is constant), the kinematic equations in the (ξ,η) plane are

$$\ddot{\xi}(t)=-\omega\dot{\eta}(t),\quad \ddot{\eta}(t)=\omega\dot{\xi}(t), \quad (7)$$

where $\ddot{\xi}(t)$ is the normal (longitudinal) acceleration and $\ddot{\eta}(t)$ denotes the tangential acceleration, and ω is the constant yaw rate (ω > 0 implies a counterclockwise turn). The tangential component of the acceleration is equal to the rate of change of the speed, that is, $\ddot{\eta}(t)=d\dot{\eta}(t)/dt=d(\omega\xi(t))/dt$, and the normal component is defined as the square of the speed in the tangential direction divided by the radius of the curvature of the path, that is, $\ddot{\xi}(t)=-\dot{\eta}^2(t)/\xi(t)=-\omega^2\xi^2(t)/\xi(t)$ where $\dot{\eta}(t)=\omega\xi(t)$. The state space representation of (7) with the state vector defined by $x(t)=[\xi(t)\ \ \dot{\xi}(t)\ \ \eta(t)\ \ \dot{\eta}(t)]'$ becomes

$$\dot{x}(t)=Ax(t), \quad (8)$$

where

$$A=\begin{bmatrix}0 & 1 & 0 & 0\\ 0 & 0 & 0 & -\omega\\ 0 & 0 & 0 & 1\\ 0 & \omega & 0 & 0\end{bmatrix}.$$

The state transient matrix of the system (8) is given by

$$e^{At}=\begin{bmatrix}1 & \frac{\sin\omega t}{\omega} & 0 & -\frac{1-\cos\omega t}{\omega}\\ 0 & \cos\omega t & 0 & -\sin\omega t\\ 0 & \frac{1-\cos\omega t}{\omega} & 1 & \frac{\sin\omega t}{\omega}\\ 0 & \sin\omega t & 0 & \cos\omega t\end{bmatrix}. \quad (9)$$

It has been remarked that if the angular rate ω in (7) is time-varying, (9) would be no longer true. In the sequel, following the approach in [1, p. 466], a "nearly" constant- speed turn model in a discrete-time domain is introduced. In this approach, the model itself is motivated from (9), but the angular rate is allowed to vary.

A new state vector by augmenting the angular rate $\omega(k)$ to the state vector of (7) is defined as follows:

$$x^a(k)=[\xi(k)\quad \dot{\xi}(k)\quad \eta(k)\quad \dot{\eta}(k)\quad \omega(k)]', \quad (10)$$

where superscript a denotes the augmented value. Then, the nearly constant-speed turn model is defined as follows [1, p. 467]:

$$x^a(k)=\begin{bmatrix}1 & \frac{\sin\omega(k-1)T}{\omega(k-1)} & 0 & -\frac{1-\cos\omega(k-1)T}{\omega(k-1)} & 0\\ 0 & \cos\omega(k-1)T & 0 & -\sin\omega(k-1)T & 0\\ 0 & \frac{1-\cos\omega(k-1)T}{\omega(k-1)} & 1 & \frac{\sin\omega(k-1)T}{\omega(k-1)} & 0\\ 0 & \sin\omega(k-1)T & 0 & \cos\omega(k-1)T & 0\\ 0 & 0 & 0 & 0 & 1\end{bmatrix}$$

$$\times x^a(k-1)+\begin{bmatrix}T^2/2 & 0 & 0\\ T & 0 & 0\\ 0 & T^2/2 & 0\\ 0 & T & 0\\ 0 & 0 & T\end{bmatrix}\nu^a(k-1). \quad (11)$$

Evidently, both (5) and (11) are special forms of (1). In addition, it is reasonable to assume that the transition between the driving modes of an ACC vehicle has the Markovian probability governed by (3). Consequently, the kinematic behaviors of an ACC vehicle can be suitably described in the framework of the stochastic hybrid systems.

3. IMM ALGORITHM FOR TRACKING

3.1. The IMM algorithm

In order to accurately track the motion of preceding vehicles in the ACC environment, an IMM algorithm is used in this paper. The concept (structure) of the IMM algorithm during one cycle is given in [1, p.454] and [14]. In this paper two models of the IMM algorithm are used: one for rectilinear motion and the other for curvilinear motion. The tracking procedure of the vehicle in a rectilinear motion using (5) is carried out by the standard Kalman filter, which is not discussed in this paper. However, for tracking curvilinear motions, which requires the estimation of ω with a new augmented model (8) in Section 2, an UKF is used. (15)

Remark 1: When target dynamics are described by multiple-switching models, the posterior density of the state vector is a mixture density [1]. The EKF approximates the mixture components with the Gaussian probability density function. The goal of the IMM algorithm is to merge all mixture components into a single Gaussian distribution in such a way that the first and the second moments are matched. The main point is that for each dynamic model a separate filter is used. In this paper, we use two Kalman- based filters for two stochastic models: one for rectilinear motion and the other for curvilinear motion. The results of these two model-matched filters are mixed before filtering. The outputs of the model-matched Kalman-based filters at time t_k include: the state estimate $\hat{x}^a(k|k)$, covariance $P^a(k|k)$ and the model probability $\mu(k)$. The overall output of the IMM algorithm is then calculated using the Gaussian mixture equations. The drawbacks of the IMM algorithm using an EKF are as follows. First, the EKF approximates a non-Gaussian density by a Gaussian density [24]. Second, the IMM algorithm approximates the Gaussian mixture by a single Gaussian density. If these assumptions break down, the IMM algorithm using an EKF may diverge.

3.2. The UKF for the constant-speed turn model

The nearly constant-speed turn model of (11) can be rewritten as follows:

$$x^a(k) = f^a[x^a(k-1), \omega(k-1)] + G(k-1)v^a(k-1), \quad (12)$$

where the function $f^a(\cdot)$ is known and remains unchanged during the estimation procedure. The noise transition matrix $G(k\text{-}1)$ is the same form as that given in (11). Because of the well-known drawbacks of the EKF, the UKF for the constant-speed turn model is used [8,21].

Similarly to the EKF, the UKF is a recursive minimum mean square error estimator. But unlike the EKF, which only uses the first-order terms in the Taylor series expansion of the non-linear measurement equation, the UKF uses the true measurement model and approximates the distribution of the state vector. This state distribution is still represented by a Gaussian density, but it is specified with a set of deterministically chosen sample (or sigma) points. The sample points completely capture the true mean and covariance of the Gaussian random vector. When propagated though any non-linear system, the sample points capture the posterior mean and covariance accurately to the second order. The main building block of the UKF is the unscented transform, described below.

The unscented transform is a method for calculating the statistics of a random vector which undergoes a non-linear transformation. Let $x \in \Re^{n_x}$ be a random vector, $p: \Re^{n_x} \to \Re^{n_y}$ a non-linear transformation and $y = p(x)$. Assume that the mean and the covariance of x are $\bar{x}$ and P_x, respectively. The procedure for calculating the first two moments of y using the unscented transform is as follows [8].

1) Compute $(2n_x + 1)$ sigma points χ_i and their weights W_i:

$$\chi_0 = \bar{x}, \quad W_0 = \frac{\kappa}{n_x + \kappa}, \quad i = 0,$$

$$\chi_i = \bar{x} + (\sqrt{(n_x + \kappa)P_x})_i, \quad W_i = \frac{1}{2(n_x + \kappa)}, \quad i = 1, \cdots, n_x,$$

$$\chi_i = \bar{x} - (\sqrt{(n_x + \kappa)P_x})_i, \quad W_i = \frac{1}{2(n_x + \kappa)}, \quad i = n_x + 1, \cdots, 2n_x, \quad (13)$$

where κ is a scaling parameter for fine tuning the higher order moments of the approximation and $(\sqrt{(n_x + \kappa)P_x})_i$ is the ith row or column of the matrix square root of $(n_x + \kappa)P_x$.

2) Propagate each sigma point through the non-linear function

$$\zeta_i = p(\chi_i) \quad (i = 0, \cdots, 2n_x). \quad (14)$$

3) Calculate the mean and covariance of y as follows:

$$\bar{y} = \sum_{i=0}^{2n_x} W_i \zeta_i,$$

$$P_y = \sum_{i=0}^{2n_x} W_i (\zeta_i - \bar{y})(\zeta_i - \bar{y})'. \quad (15)$$

Using the unscented transformation, the UKF equations for the constant-speed turn model are given in Fig. 3. Note that the UKF requires the computation of a matrix square root in (13), which can be performed using the Cholesky factorization.

Remark 2: In the unscented transformation, on which the UKF is based, a set of weighted sigma points are deterministically chosen so that certain properties of these points match those of the prior distribution. Each point is then propagated through a non-linear function and the properties of the transformed set are calculated. With this set of points, the unscented transform guarantees the same performance as the truncated second order Gaussian filter, with the same order of calculations as an EKF but without the need to calculate Jacobians.

4. SIMULATIONS RESULTS

As described in this section, we considered a state estimation problem of a vehicle in two dimensions. Simulations were executed to compare the performance of both IMM algorithms with the EKF and the UKF, respectively, for curvilinear motions. The performance of the two algorithms was compared with the use of Monte Carlo simulations. The maneuvering vehicle trajectories were generated using the various patterns mentioned in Section 2.1. Two kinematic models were used to track the maneuvering vehicle: A constant-velocity model for rectilinear motion and a constant-speed turn model for curvilinear motion. We then compare the performance of two different IMM algorithms with these two models.

4.1. The driving scenarios

It was assumed that the vehicle moves rectilinearly in the beginning. The target initial positions and velocities were differently set for each scenario. The single-target track of the maneuvering vehicle was also assumed to have been previously initialized and that track maintenance was the goal of the IMM algorithms. The results for 4 selected scenarios are presented, according to the driving patterns, in Fig. 2.

i) Scenario for straight line and curve: The target initial positions and velocities were (x_0 = 0 m, y_0 = 0 m, $\dot{x}_0$ = 28 m/s, $\dot{y}_0$ = 28 m/s, ω = 0°). Its trajectory was a constant velocity between 0 s and 19 s with a speed of 28 m/s; a turn with a constant yaw rate of ω = 3.74 °/s between 20 s and 59 s; a constant velocity between 60 s and 89 s; a turn with a constant yaw rate of ω = 3.74 °/s between 90 s and 129 s; a constant velocity between 130 s and 149 s; a turn with a constant yaw rate of ω = 3.74 °/s between 150 s and 200 s.

ii) Cut-in/out scenario: The target initial positions and velocities were (x_0 = 0 m, y_0 = 20 m, $\dot{x}_0$ = 28 m/s, $\dot{y}_0$ = 0 m/s, ω = 0°). Its trajectory was a straight line between 0 s and 19 s with a speed of 28 m/s; a turn with a constant yaw rate of ω = 3.74 °/s between 20 s and 39 s; a constant velocity between 40 s and 41 s with a speed of 28 m/s; a turn between 42 s and 63 s with a yaw rate of ω = 3.74 °/s; a straight line between 64 s and 134 s with a speed of 28 m/s; a turn with a constant yaw rate of ω = 3.74 °/s between 135 s and 154 s; a constant velocity between 155 s and 159 s with a speed of 28 m/s; a turn between 160 s and 179 s with a yaw rate of ω = 3.74 °/s and a straight line between 180 s and 200 s.

iii) U-turn scenario: The target initial positions and velocities were (x_0 = 10 m, y_0 = 10 m, $\dot{x}_0$ = 28 m/s, $\dot{y}_0$ = 0 m/s, ω = 0°). This scenario included

Initialization: $\hat{x}^a(0|0)$, $P^a(0|0)$ with $k = 1$

Sigma points and weights:

$\chi_i(k-1|k-1)$, W_i $(i = 0,\cdots,2n)$

Time-update equations:

predicted sigma points

$$\chi_i(k|k-1) = f^a[\chi_i(k-1|k-1), \omega(k-1)]$$

predicted mean and covariance

$$\hat{x}^a(k|k-1) = \sum_{i=0}^{2n} W_i \chi_i(k|k-1),$$

$$P^a(k|k-1) = Q^a + \sum_{i=0}^{2n} W_i[\chi_i(k|k-1) - x^a(k|k-1)][\chi_i(k|k-1) - x^a(k|k-1)]'$$

predicted measurement sigma points

$$\Im_i(k|k-1) = h[\chi_i(k|k-1), \omega(k)]$$

predicted measurement

$$\hat{z}^a(k|k-1) = \sum_{i=0}^{2n} W_i \Im_i(k|k-1)$$

Measurement-update equations:

measurement covariance

$$P_{zz}^a = R(k) + \sum_{i=0}^{2n} W_i[\Im_i(k|k-1) - \hat{z}^a(k|k-1)] \times [\Im_i(k|k-1) - \hat{z}^a(k|k-1)]'$$

$$P_{xz}^a = \sum_{i=0}^{2n} W_i[\chi_i(k|k-1) - \hat{x}^a(k|k-1)] \times [\Im_i(k|k-1) - \hat{z}^a(k|k-1)]'$$

filter gain

$$K^a(k) = P_{xz}^a (P_{zz}^a)^{-1}$$

mean and covariance

$$\hat{x}^a(k|k) = \hat{x}^a(k|k-1) + K^a(k)[z(k) - \hat{z}^a(k|k-1)]$$

$$P^a(k|k) = P^a(k|k-1) - K^a(k) P_{zz}^a K'^a(k)$$

Fig. 3. UKF equations for the constant speed turn model.

a non-maneuvering driving mode during scans from 1 s to 60 s with a speed of 28 m/s, a 180 ° -turn, lasting from scan 61 s to 145 s with a yaw rate of ω = 3.74 °/s , and a non-maneuvering driving mode from scan 146 s to 200 s.

iv) Interchange scenario: The target initial positions and velocities were (x_0 = 0 m, y_0 = 0 m, $\dot{x}_0$ = 28 m/s, $\dot{y}_0$ = 0 m/s, ω = 0°). This scenario included a non-maneuvering driving mode during scans from 1 s to 40 s with a speed of 28 m/s, a 270° -turn, lasting from scan 41 s to 168 s with a yaw rate of ω = 3.74 °/s , and a non-maneuvering driving mode from scan 169 s to 200 s. The maneuvering vehicle speed was 28 m/s.

4.2. Parameters used in the design

The parameters used in the design are listed here. Subscripts "CV" and "CST" stand for "constant velocity" and "constant speed turn," respectively. The initial yaw rate of the driving scenarios was $\omega(0)$ = 3 °/s . The error covariances of the initial state and covariances of process noise were as follows:

CV mode: $P^{\mathrm{KF}}(0) = \mathrm{diag}\{100 \;\; 100 \;\; 100 \;\; 100\}$,

$$Q^{\mathrm{KF}} = (0.001)^2 \mathrm{I} ,$$

CST mode: $P^{\mathrm{EKF}}(0) = P^{\mathrm{UKF}}(0)$

$$= \mathrm{diag}\{100 \;\; 100 \;\; 100 \;\; 100 \;\; \sigma_\omega^2\} ,$$

$Q^{\mathrm{EKF}} = Q^{\mathrm{UKF}} = \mathrm{diag}\{(0.25)^2 \;\; (0.25)^2 \;\; (0.25)^2 \;\; (0.25)^2 \;\; \sigma_\omega^2\}$

where $\sigma_\omega = (0.01)°/\mathrm{s}$. The measurement noise covariance matrix was calculated as $\sigma_\xi = 10\mathrm{m}$ and $\sigma_\eta = 10\mathrm{m}$.

The transition probabilities for the IMM algorithms using the EKF and the UKF, respectively, were represented in the Markov chain transition matrix

$$\pi_{ij}^{\mathrm{EKF}} = \pi_{ij}^{\mathrm{UKF}} = \begin{bmatrix} 0.95 & 0.05 \\ 0.05 & 0.95 \end{bmatrix} \pi_{ij} .$$

The initial mode probability vectors μ were chosen as follows:

$$\mu^{\mathrm{EKF}} = \mu^{\mathrm{UKF}} = \begin{bmatrix} 0.5 \\ 0.5 \end{bmatrix} .$$

4.3. Performance evaluation and analysis

The RMSE of each state component was chosen as the measure of performance. The performance of the IMM algorithm with an EKF and that of the IMM algorithm with an UKF are shown in Fig. 4 - Fig. 11, where the RMSE in the position and the velocity are plotted. The results presented here are based on 100 Monte Carlo runs. First of all, it is evident that the suggested algorithm has almost equal position and velocity estimation accuracy for all scenarios. The

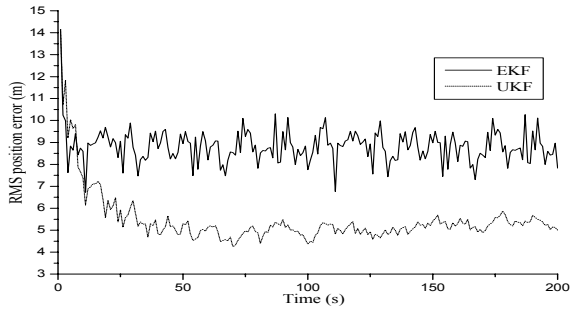

Fig. 4. Comparison of the position errors in the case of straight lines and curves.

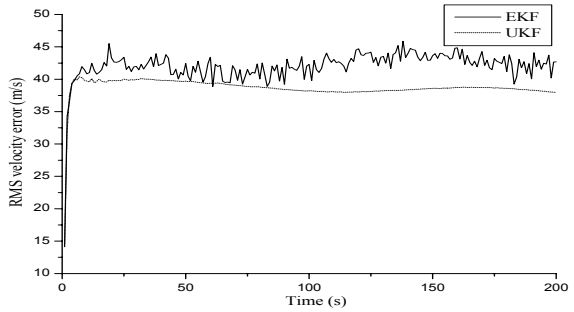

Fig. 5. Comparison of the velocity errors in the case of straight lines and curves.

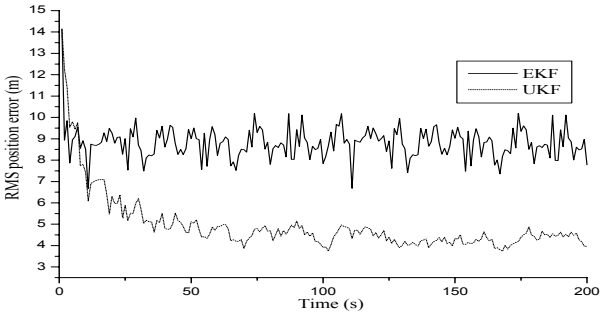

Fig. 6. Comparison of the position errors in the case of cut-in/out.

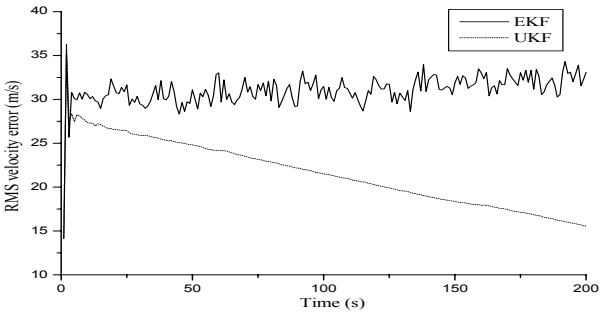

Fig. 7. Comparison of the velocity errors in the case of cut-in/out.

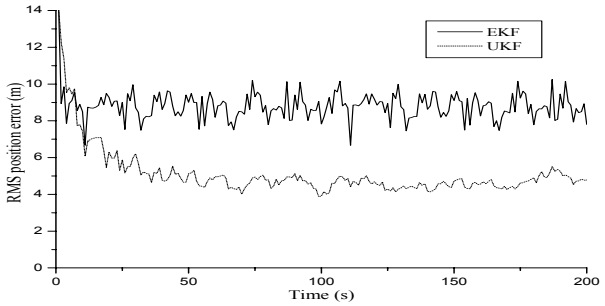

Fig. 8. Comparison of the position errors in the case of u-turn.

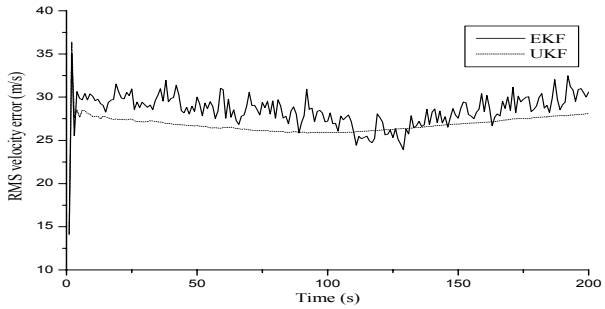

Fig. 9. Comparison of the velocity errors in the case of u-turn.

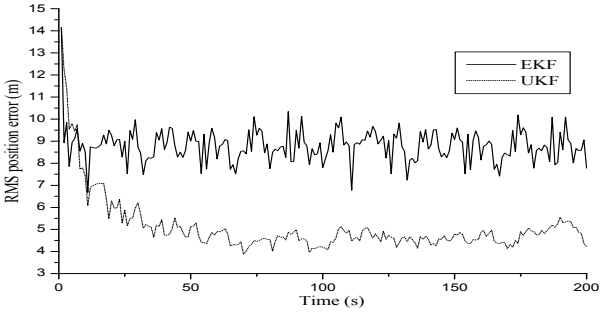

Fig. 10. Comparison of the position errors in the case of interchange.

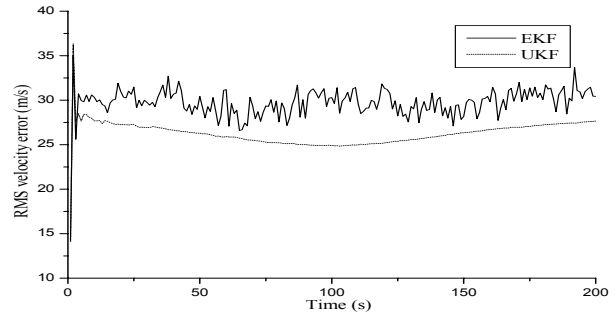

Fig. 11. Comparison of the velocity errors in the case of interchange.

position RMSE of the IMM with an UKF is evidently superior to that of the IMM with an EKF. This is because, unlikely EKF, UKF does not approximate nonlinear functions but directly propagates mean and covariance through the nonlinear system equation. In addition, the IMM algorithm with an UKF is characterized by lower-peak dynamic errors and a shorter response time. These conclusions were confirmed by the RMSE plot presented in Figs. 4-11, respectively.

5. CONCLUSIONS

In this paper, an interacting multiple model algorithm with an UKF, as a tracking algorithm, to track maneuvering vehicles on a road was designed. As models to track the maneuvering vehicles, two kinematic models were derived: The constant velocity model for linear motion and the constant-speed turn model for curvilinear motion. For constant-speed turn model, an unscented Kalman filter was used because of the drawbacks of the extended Kalman filter in nonlinear systems. The suggested algorithm reduced the root mean square error for linear motions, and it could rapidly detect possible turning motions.

REFERENCES

[1] Y. Bar-Shalom, X. Li, and T. Kirubarajan, *Estimation with Applications to Tracking and Navigation*, John Wiley & Sons, INC, New York, Chapter 11, pp. 421-490, 2001.

[2] D. S. Caveney, *Multiple Target Tracking in the Adaptive Cruise Control Environment Using Multiple Models and Probabilistic Data Association*, M. S. Thesis, University of California, Berkeley, U. S. A., 1999.

[3] Z. Ding, H. Leung, K. Chan, and Z. Zhu, "Model-set adaptation using a fuzzy Kalman filter," *Mathematical and Computer Modelling*, vol. 34, no. 7-8, pp. 799-812, October 2001.

[4] F. Dufour and M. Mariton, "Passive sensor data fusion and maneuvering target tracking," in: Y. Bar-Shalom (Ed.), *Multitarget-Multisensor Tracking: Applications and Advances*, Artech House, Norwood, MA, Chapter 3, pp. 65-92, 1992.

[5] J. P. Helferty, "Improved tracking of maneuvering targets: The use of turn-rate distributions for acceleration modeling," *IEEE Trans. on Aerospace and Electronic Systems,* vol. 32, no. 4, pp. 1355-1361, October 1996.

[6] A. Houles and Y. Bar-Shalom, "Multisensor tracking of a maneuvering target in clutter," *IEEE Trans. on Aerospace and Electronic Systems,* vol. 25, no. 2, pp. 176-189, March 1989.

[7] V. P. Jilkov, D. S. Angelova, TZ. A. Semerdjiev, "Design and comparison of mode-set adaptive

IMM algorithms for maneuvering target tracking," *IEEE Trans. on Aerospace and Electronic Systems,* vol. 35, no. 1, pp. 343-350, January 1999.

[8] S. J. Julier, J. K. Uhlmann, and H. F. Durrant-Whyte, "A new method for the nonlinear transformation of means and covariances in filters and estimators," *IEEE Trans. on Automatic Control,* vol. 45, no. 3, pp. 477-482, March 2000.

[9] Y. S. Kim and K. S. Hong, "A suboptimal algorithm of the optimal Bayesian filter based on the receding horizon strategy," *International Journal of Control, Automation, and Systems*, vol. 1, no. 2, pp. 163-170, June 2003.

[10] J. Ph. Lauffenburger, M. Basset, F. Coffin, and G. L. Gissinger, "Driver-aid system using path-planning for lateral vehicle control," *Control Engineering Practice*, vol. 11, no. 2, pp. 217-231, February 2003.

[11] B. J. Lee, Y. H. Joo, and J. B. Park, "An Intelligent tracking method for a maneuvering target," *International Journal of Control, Automation, and Systems*, vol. 1, no. 1, pp. 93-100, March 2003.

[12] T. G. Lee, "Centralized Kalman filter with adaptive measurement fusion: its application to a GPS/SDINS integration system with an additional sensor," *International Journal of Control, Automation, and Systems*, vol. 1, no. 4, pp. 444-452, December 2003.

[13] X. Li and Y. Bar-Shalom, "Multiple-model estimation with variable structure," *IEEE Trans. on Automatic Control,* vol. 41, no. 4, pp. 478-493, April 1996.

[14] X. Li and Y. Bar-Shalom, "Design of an interacting multiple model algorithm for air traffic control tracking," *IEEE Trans. on Control Systems Technology,* vol. 1, no. 3, pp. 186-194, September 1993.

[15] E. Mazor, A. Averbuch, Y. Bar-Shalom, and J. Dayan, "Interacting multiple model methods in target tracking: A survey," *IEEE Trans. on Aerospace and Electronic Systems,* vol. 34, no. 1, pp. 103-123, January 1998.

[16] S. McGinnity and G. W. Irwin, "Fuzzy logic approach to manoeuvring target tracking," *IEE Proceedings on Radar, Sonar, and Navigation*, vol. 145, no. 6, pp. 337-341, December 1998.

[17] I. K. Moon and K. S. Yi, "Vehicle tests of a longitudinal control law for application to stop-and-go cruise control," *KSME International Journal*, vol. 16, no. 9, pp. 1166-1174, 2002.

[18] A. Munir and D. P. Atherton, "Adaptive interacting multiple model algorithm for tracking a manoeuvring target," *IEE Proceedings on Radar, Sonar, and Navigation*, vol. 142, no. 1, pp. 11-17, February 1995.

[19] N. Nabaa and R. H. Bishop, "Validation and comparison of coordinated turn aircraft maneuver models," *IEEE Trans. on Aerospace and Electronic Systems,* vol. 36, no. 1, pp. 250-259, January 2000.

[20] R. Rajamani, C. Zhu, and L. Alexander, "Lateral control of a backward driven font-steering vehicle," *Control Engineering Practice*, vol. 11, no. 5, pp. 531-540, May 2003.

[21] B. Ristic and M. S. Arulampalam, "Tracking a manoeuvring target using angle-only measurements: algorithms and performance," *Signal Processing*, vol. 83, no. 6, pp. 1223-1238, June 2003.

[22] E. Semerdjiev and L. Mihaylova, "Variable- and fixed-structure augmented interacting multiple-model algorithms for manoeuvring ship tracking based on new ship models," *International Journal of Applied Mathematics and Computer Science*, vol. 10, no. 3, pp. 591-604, 2000.

[23] I. Simeonova and T. Semerdjiev, "Specific features of IMM tracking filter design," *An International Journal of Information and Security*, vol. 9, pp. 154-165, 2002.

[24] W. I. Tam, K. N. Plataniotis, and D. Hatzinakos, "An adaptive Gaussian sum algorithm for radar tracking," *Signal Processing*, vol. 77, no. 1, pp. 85-104, August 1999.

Yong-Shik Kim was born in Busan, Korea, on November 24, 1970. He received the B.S. degree in Mechanical Engineering from Donga University, Busan, Korea, in 1994 and the M.S. degree in Mechanical and Intelligent Systems Engineering from Pusan National University, Busan, Korea, in 2000. He is now a Ph.D. candidate in the Department of Mechanical and Intelligent Systems Engineering at Pusan National University, Busan, Korea. His research interests include estimation theory, target-tracking systems, sensor fusion, and fault detection.

Keum-Shik Hong, for photograph and biography, see p. 67 of the March 2004 issue of this journal.